



Research Internship Abroad (BEPE/FAPESP)

Remote Sensing Anomaly Detection in Time-Series Imagery and Application Development in the Agricultural Context

Process: 2025/22483-0

Final Report: December/01/2025 to March/01/2026 (3 months)

Brazil Advisor: Dr. Rubens Augusto Camargo Lamparelli
UK Supervisor: Dr. Jefersson Alex dos Santos
UK Co-Supervisor: Prof. Po Yang
Fellow: Fernando Kenzo Imami Fugihara

Campinas, SP
2025

Abstract

This report documents the theoretical foundations, methodological approaches, and findings from the the internship (December 1 - March 1), focusing on time-series analysis fundamentals, anomaly detection algorithms.

Contents

1	Introduction	4
1.1	Research Context and Objectives	4
2	Time-Series Analysis Fundamentals	5
2.1	Time-Series Definitions	5
2.1.1	Univariate Time-Series (UTS)	5
2.1.2	Multivariate Time-Series (MTS)	5
2.2	Time-Series Components	5
2.2.1	Level	5
2.2.2	Stationarity	6
2.2.3	Trend	6
2.2.4	Seasonality	6
2.2.5	Cyclicity	6
2.3	Time-Series Smoothing Techniques	6
2.3.1	Moving Average and Weighted Average	7
2.3.2	Single Exponential Smoothing (SES)	7
2.3.3	Double Exponential Smoothing (DES)	8
2.3.4	Triple Exponential Smoothing (TES) / Holt-Winters	8
2.4	Anomalies in Time-Series	9
2.4.1	Pest-Related Anomalies	9
3	Methodology	9

3.1	Data and Study Regions	9
3.1.1	Mossoró, Rio Grande do Norte, Brazil	9
3.1.2	Ejura, Ghana, West Africa	10
3.1.3	Kurnool and Gadwal Districts, Southern India	11
3.2	Preprocessing Sentinel-2 Imagery	12
3.3	Spectral Indices	12
3.3.1	Plastic Indices	13
3.3.2	Vegetation Indices	13
3.4	Time-Series Representation and Smoothing	13
3.5	Proposed anomaly detection model	14
3.5.1	Problem Formulation	14
3.5.2	Baseline Time-Series Modeling	14
3.5.3	Anomaly Scoring	14
3.6	Evaluation Metrics	14
4	Results and Discussion	15
4.1	Proof of Concept: Plastic deterioration detection in Mossoró with Sentinel-2	15
4.2	Proof of Concept: FAW infestation detection in Southern India with Sentinel-2	15
4.2.1	Spectral Signatures of Pest Infestation	15
4.2.2	Time-Series Vegetation Indexes Analysis	17
4.2.3	Temporal Anomaly Detection	19
5	Conclusion and Future Work	20

1 Introduction

1.1 Research Context and Objectives

This research internship focuses on the detection of anomalies in agricultural systems using time-series analysis of Sentinel-2 satellite imagery. The primary objectives are:

- **Proof of Concept:** Verify if it's possible to detect pest-net installations in plasticulture systems in Mossoró, Brazil, using time-series analysis of Sentinel-2 imagery.
- **Proof of Concept:** Verify if it's possible to detect pest infestations, such as Fall Army-worm (*Spodoptera frugiperda*) in maize crops, using time-series analysis of Sentinel-2 imagery.
- **Algorithm Development:** Model anomaly detection algorithms capable of identifying both pest-net installations and pest infestation events in time-series satellite imagery.

In the context of learning anomaly detection techniques applied to remote sensing, the research objectives also align with the Brazil–UK–Africa collaboration “SmartPest-Ghana: Exploring LLM-driven mobile solutions for climate-smart pest management in maize farming”, funded by UK Research and Innovation (UKRI).

In terms of application development, the internship aims to contribute to the development of a mobile application that leverages the anomaly detection algorithms to provide real-time pest management recommendations to smallholder farmers in Ghana.

- **Application Development:** Contribute to the development of a mobile application that integrates the Computer Vision and LLM models to provide real-time pest management recommendations to smallholder farmers.

2 Time-Series Analysis Fundamentals

2.1 Time-Series Definitions

2.1.1 Univariate Time-Series (UTS)

A univariate time-series represents a single variable (such as NDVI) measured at a single pixel location over time. For a pixel observed at t timestamps, the UTS X is represented as:

$$X = (x_1, x_2, \dots, x_t)$$

where x_i represents the feature value at timestamp $i \in T$ and $T = \{1, 2, \dots, t\}$.

2.1.2 Multivariate Time-Series (MTS)

A multivariate time-series represents multiple variables that exhibit both temporal dependencies (correlations across time) and spatial dependencies (correlations between variables). For a pixel with d features observed over t timestamps:

$$X = (X_1, X_2, \dots, X_t) = \left((x_1^1, x_1^2, \dots, x_1^d), (x_2^1, x_2^2, \dots, x_2^d), \dots, (x_t^1, x_t^2, \dots, x_t^d) \right) \quad (1)$$

where $X_i = (x_i^1, x_i^2, \dots, x_i^d)$ represents the feature vector at time i , and x_i^j is the observation at time i for the j -th dimension.

2.2 Time-Series Components

Understanding the structural components of time-series data is essential for selecting appropriate analysis and smoothing techniques.

2.2.1 Level

The level represents the average value of the time-series and can be conceptualized as the mean around which observations fluctuate.

2.2.2 Stationarity

A time-series is stationary when its statistical properties (mean, variance, covariance) remain constant over time. Stationarity is an important assumption for many time-series analysis techniques.

2.2.3 Trend

The trend captures long-term systematic increases or decreases in the series. Presence of trend typically violates stationarity, as the mean changes over time.

2.2.4 Seasonality

Seasonality refers to regular, predictable patterns that repeat at fixed intervals (e.g., daily, weekly, seasonal cycles in crop development).

2.2.5 Cyclicity

Cycles are repetitive patterns similar to seasonality but occurring over longer, less predictable time periods not aligned with calendar intervals. In agricultural contexts, cycles may relate to multi-year climate patterns or economic factors.

2.3 Time-Series Smoothing Techniques

Smoothing techniques are essential preprocessing steps that remove noise from time-series data while preserving important patterns. This is particularly critical when comparing pixel time-series or applying distance-based algorithms.

Consider two pixels with similar underlying patterns but different noise characteristics. Without smoothing, distance-based clustering algorithms may incorrectly classify these pixels as dissimilar due to noise rather than genuine differences in behavior. Smoothing addresses this issue by enhancing signal-to-noise ratio.

The choice of smoothing method depends on the structural characteristics of the time-series, as summarized in Table 1.

Table 2 defines the variables used in smoothing formulations.

Table 1: Smoothing algorithm applicability for different time-series structures

Algorithm	Level	Trend	Seasonality	Parameters
Single HWES	Yes	No	No	α
Double HWES	Yes	Yes	No	α, β
Triple HWES	Yes	Yes	Yes	α, β, γ

Table 2: Variables utilized in smoothing models

Symbol	Description
X	Observation
S	Smoothed observation
B	Trend factor
C	Seasonal index
F	Forecast at m periods ahead
α	Data smoothing factor, $\alpha \in (0, 1)$
β	Trend smoothing factor, $\beta \in (0, 1)$
γ	Seasonal change smoothing factor, $\gamma \in (0, 1)$
ϕ	Damped smoothing factor, $\phi \in (0, 1)$
t	Time period index

2.3.1 Moving Average and Weighted Average

These methods compute the future value as the average (or weighted average) of k previous values. While useful for trend observation and feature engineering, these approaches are unsuitable for satellite time-series with trend and seasonality components.

2.3.2 Single Exponential Smoothing (SES)

SES models the level component only and is appropriate for stationary series without trend or seasonality. It weights recent observations more heavily based on the assumption that the future is more closely related to the recent past.

$$S_0 = X_0$$

$$S_t = \alpha X_t + (1 - \alpha)S_{t-1}, \quad t > 0, \quad 0 < \alpha < 1$$

Application: Limited applicability to agricultural time-series, which typically exhibit both trend and seasonality.

2.3.3 Double Exponential Smoothing (DES)

DES extends SES by incorporating trend, making it suitable for series with trend but without seasonality.

$$\begin{aligned} S_0 &= X_0 \\ B_0 &= X_1 - X_0 \\ S_t &= \alpha X_t + (1 - \alpha)(S_{t-1} + B_{t-1}) \\ B_t &= \beta(S_t - S_{t-1}) + (1 - \beta)B_{t-1}, \quad \alpha, \beta \in (0, 1) \end{aligned}$$

Application: Applicable to agricultural time-series when seasonality is not a dominant factor.

2.3.4 Triple Exponential Smoothing (TES) / Holt-Winters

TES represents the most comprehensive smoothing approach, modeling level, trend, and seasonality simultaneously. This method is most appropriate for agricultural satellite time-series, which exhibit all three components.

$$\begin{aligned} S_0, F_0 &= X_0 \\ B_0 &= \frac{\sum_{i=0}^{L-1} (X_{L+i} - X_i)}{L^2} \\ S_t &= \alpha(X_t - C_{t \bmod L}) + (1 - \alpha)(S_{t-1} + \phi B_{t-1}) \\ B_t &= \beta(S_t - S_{t-1}) + (1 - \beta)\phi B_{t-1} \\ C_{t \bmod L} &= \gamma(X_t - S_t) + (1 - \gamma)C_{t \bmod L} \\ F_{t+m} &= S_t + B_t \sum_{i=1}^m \phi^i + C_{t \bmod L}, \quad \alpha, \beta, \gamma \in (0, 1) \end{aligned}$$

Application: Recommended for Sentinel-2 vegetation index time-series, which exhibit clear seasonal patterns related to crop phenology.

2.4 Anomalies in Time-Series

According to Hawkins et al (1980) an anomaly is a data point or sequence that deviates from the general data distribution. In a time-series dataset, only a small fraction contains anomalies, where the majority of the data points follow expected patterns. In remote-sensing data, there is a lot of different informations that deviate from normality, such as sensor noise, atmospheric effects, cloud cover, seasonal variations, and landscape complexity (Fu et al., 2025). The most meaningful deviations are usually those that are significantly different from the norm.

Anomalies in UTS and MTS can be classified as temporal, intermetric, or temporal-intermetric anomalies (Li et al., 2021). Temporal anomalies can be compared with either their neighbours (local) or the whole time series (global), and they present different forms depending on their behaviour (Lai et al., 2022). In our case, we want to detect pest-related anomalies in agricultural fields, which is a temporal anomaly

2.4.1 Pest-Related Anomalies

3 Methodology

3.1 Data and Study Regions

This research utilizes Harmonized Sentinel-2 (S2) Level-2A surface reflectance imagery, accessed through Google Earth Engine (GEE). The Copernicus Sentinel-2 mission consists of two polar-orbiting satellites (2A and 2B) operating in sun-synchronous orbit at 786 km altitude, phased 180° apart.

3.1.1 Mossoró, Rio Grande do Norte, Brazil

The study area is located in Mossoró, Rio Grande do Norte, Brazil, where previous field assessments and local expertise provide a solid foundation for this research. The region is particularly notable for its extensive use of plasticulture in melon cultivation, making it a relevant and representative site for analyzing agricultural land-cover dynamics. Additionally, pest-management practices, such as the use of pest nets, are commonly employed to protect melon crops. Field observations conducted by the research team also confirmed that plastic mulch is often reused across multiple cultivation cycles, resulting in areas with visibly deteriorated plastic materials. Figure 1 illustrates the landscape characteristics of this region.

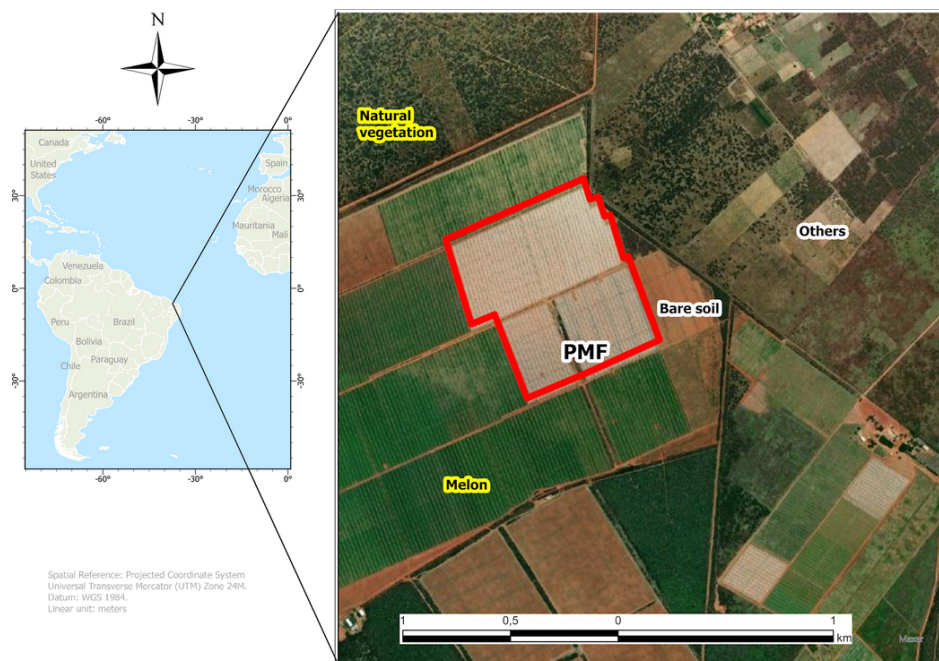


Figure 1: Mossoró study region, Rio Grande do Norte, Brazil, showing plasticulture fields.

3.1.2 Ejura, Ghana, West Africa

Figure 2 presents the diverse agricultural landscape of Ejura.

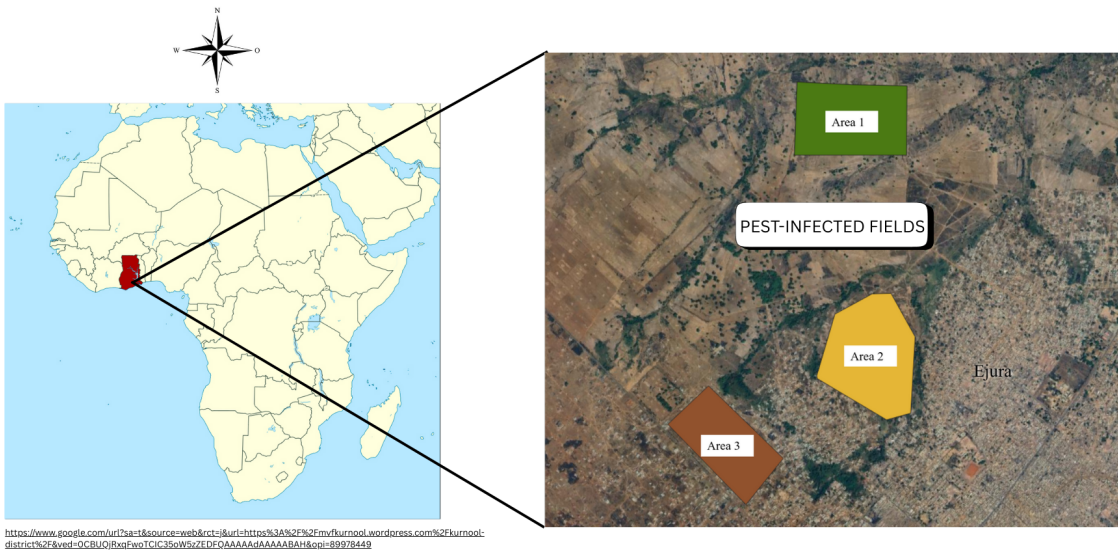


Figure 2: Ejura study region, Ghana, West Africa, showing diverse crop systems.

3.1.3 Kurnool and Gadwal Districts, Southern India

Prabhakar et al. (2022) conducted field surveys in Kurnool and Gadwal districts of Southern India to map FAW infestations in maize crops (sorghum). In his field surveys, he mapped the regions as healthy, low, medium, and severe infestation levels. Based on that, we selected one field classified as severe infestation for our proof of concept. The Prabhakar et al. (2022) field survey confirmed that the FAW infestation occurred between October 26, 2018 and November 15, 2018. Figure 3 shows the agricultural landscape characteristics of these districts.

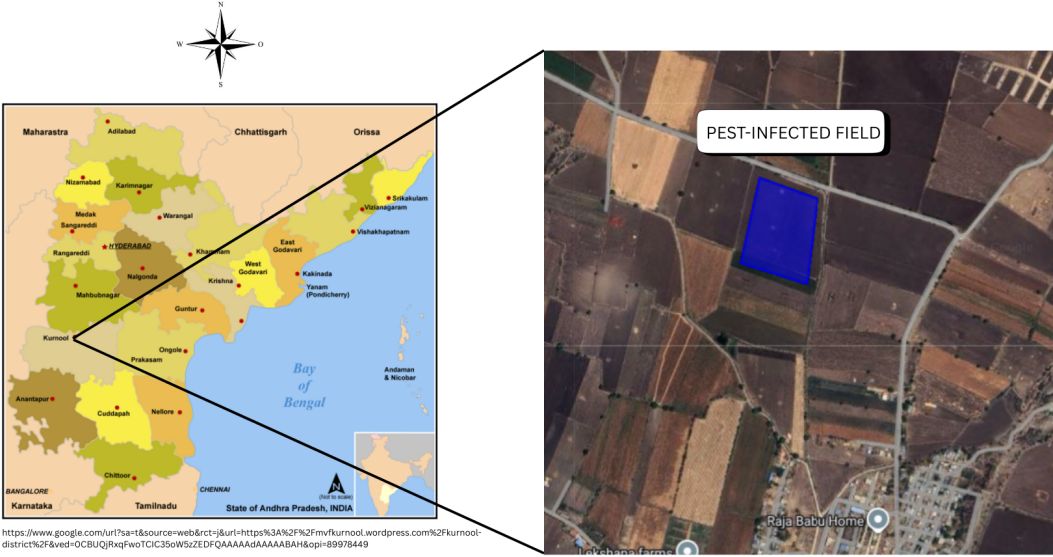


Figure 3: Kurnool and Gadwal districts, Southern India, showing maize cultivation areas.

3.2 Preprocessing Sentinel-2 Imagery

Preprocessing is a crucial step in machine learning and data pipelines (Tawakuli et al., 2025). It employs various techniques to ensure that the data fed into a model is clean, consistent, and informative, which directly influences its performance and reliability (Zheng et al., 2021). This is especially important in RSAD modeling. In RS imagery, data quality can be compromised by factors such as Earth's geometric effects resulting from its curvature and rotation, atmospheric conditions like cloud cover, sensor noise, seasonal variations, and landscape complexity (Fu et al., 2025).

3.3 Spectral Indices

Spectral vegetation indices (SVI) derived from remote sensing data provide quantitative measures of crop health and stress. These indices are particularly effective for detecting impacts of diseases and pest invasions. This research employs multiple indices to capture different aspects of plant health:

3.3.1 Plastic Indices

Table 3 summarizes the plastic indices used to detect plasticulture systems

Table 3: Spectral plastic indices and corresponding equations using Sentinel-2 bands.

Index	Equation	Reference
Plastic Index	$\frac{SWIR-NIR}{SWIR+NIR}$	Mudereri et al., 2022

3.3.2 Vegetation Indices

Studies from Dzurune et al. (2025), Bilintoh et al. (2019), Prabhakar et al. (2022), have demonstrated the effectiveness of Normalized Difference Vegetation Index (NDVI) Enhanced Vegetation Index (EVI) and Leaf Area Index (LAI), respectively, in detecting pest infestations. Table 4 presents the spectral indices used in this research, along with their mathematical formulations.

Table 4: Spectral vegetation indices and corresponding equations using Sentinel-2 bands.

Index	Equation	Reference
NDVI	$\frac{NIR-Red}{NIR+Red}$	Rouse et al., 1974
EVI	$2.5 \frac{NIR-R}{NIR+6R-7.5B+1}$	Huete et al., 1997
LAI	$3.618 \times EVI - 0.118$	Boegh et al., 2002

3.4 Time-Series Representation and Smoothing

In this study, we used a Multivariate Time-Series (MTS) representation, where each field is represented by multiple spectral indices (NDVI, LAI) over time. This approach captures both temporal dynamics and inter-index relationships. Given a field observed over t timestamps, each vector at time i , X_i , contains 2 features (spectral indices):

$$X = (X_1, X_2, \dots, X_t) = ((x_1^1, x_1^2), (x_2^1, x_2^2), \dots, (x_t^1, x_t^2)) \quad (2)$$

Where $X_i = (x_i^1, x_i^2)$ represents the feature vector at time i , with x_i^1 as NDVI and x_i^2 as LAI.

As for smoothing the time-series, we applied Triple Exponential Smoothing (TES) / Holt-Winters, which effectively models level, trend, and seasonality components present in agricultural satellite time-series.

3.5 Proposed anomaly detection model

We are proposing a AD time-series model that can detect peset infestations in agricultural fields using Sentinel-2 imagery.

3.5.1 Problem Formulation

3.5.2 Baseline Time-Series Modeling

3.5.3 Anomaly Scoring

3.6 Evaluation Metrics

4 Results and Discussion

4.1 Proof of Concept: Plastic deterioration detection in Mossoró with Sentinel-2

4.2 Proof of Concept: FAW infestation detection in Southern India with Sentinel-2

To validate whether S2 time-series can capture FAW infestation, we followed the methodology proposed by Prabhakar et al. (2022) which analyzed S2 time-series to detect FAW infestation in maize crops in Southern India. Prabhakar et al. (2022) utilized ground truth data from field surveys to classify infestation severity levels (healthy, mild, moderate, severe) and correlated these with spectral signatures and vegetation index time-series derived from S2 imagery. In its field surveys, Prabhakar et al. (2022) mapped FAW infestation dated from October 26, 2018 to November 15, 2018, these dates and a severe field were selected for our proof of concept.

4.2.1 Spectral Signatures of Pest Infestation

Based on the severity classification framework proposed by Prabhakar et al. (2022), FAW damage is categorized into four levels: healthy (Grade-1), low (Grade-2), medium (Grade-3), and severe (Grade-4) infestation. In our study, we used the severe cases of the Prabhakar et al. (2022) field survey data available only at two key moments: a pre-infestation survey, representing healthy crop conditions, and a post-infestation survey, corresponding to severe FAW damage. These two surveys were used as temporal anchors to characterize the spectral response of maize crops before and after the pest outbreak. Figure 4 illustrates the contrast between pre-attack and post-attack conditions, highlighting notable changes in reflectance patterns associated with vegetation stress caused by FAW infestation.

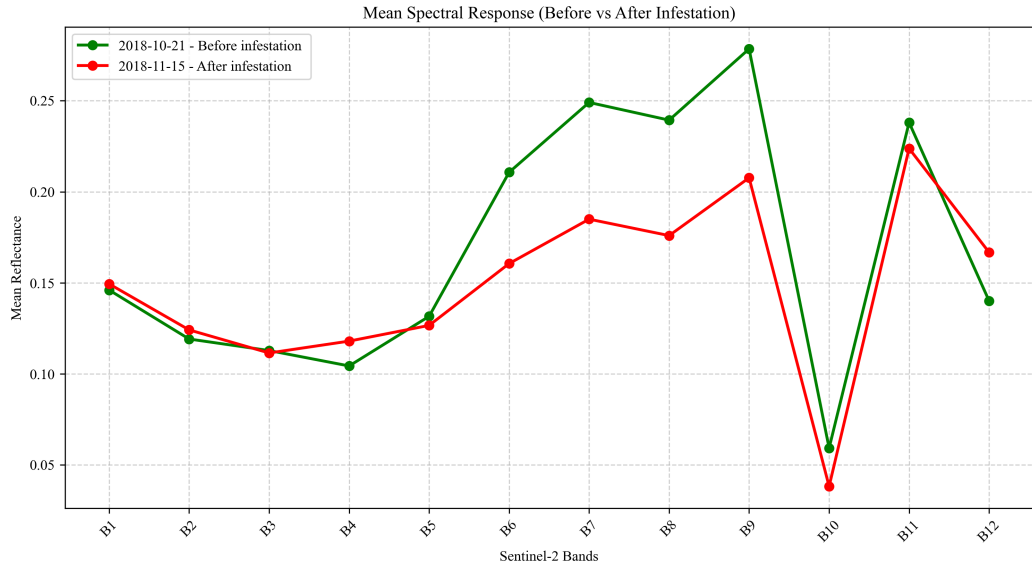


Figure 4: Spectral response of maize crops before and after Fall Armyworm infestation in Southern India.

However, ground-truth severity assessments were not available for the intermediate observation dates within the study period. To address this limitation, we adopted a temporal interpolation strategy using the available pre- and post-infestation field observations. For dates falling between these two assessment points, infestation severity was classified into two intermediate levels: low and medium, based on their temporal position in the time series and the magnitude of spectral changes observed in the satellite imagery. This approach assumes a gradual intensification of FAW damage over time and enables the representation of the dynamic evolution of infestation across the growing season, despite the absence of continuous ground-based severity monitoring. The resulting spectral signatures associated with each severity level are presented in Figure 5.

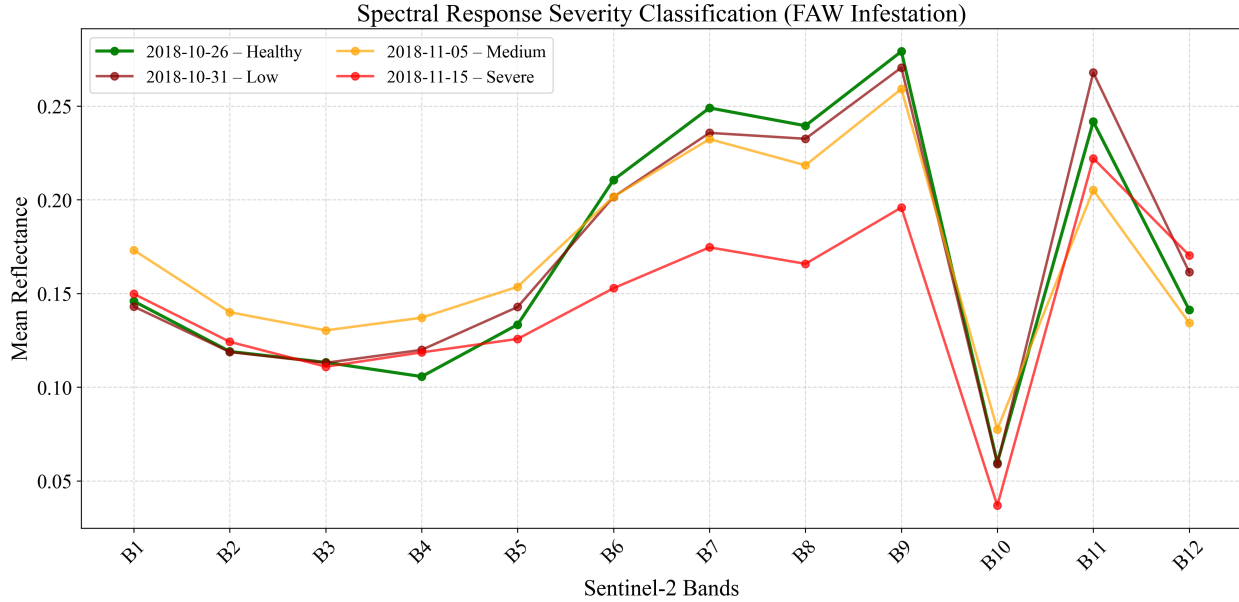


Figure 5: Spectral signatures of maize crops under different severity levels of Fall Armyworm infestation in Southern India.

Based on the mean spectral response of the field illustrated in Figure 5, we can interpret its results based on each spectral band characteristics. Near-Infrared (B8): carries information about leaf structure. Damage from pest feeding reduces reflectance in this band. Blue (B2) and Red (B4) carry chlorophyll information. Chlorophyll absorbs these wavelengths; reduction in absorption indicates decreased photosynthetic activity, often caused by pest feeding on leaves. Shortwave Infrared (B10-B12) are sensitive to water content. Pest-damaged plants often exhibit water stress, detectable in these bands.

Harvest events cause abrupt transitions from high NDVI (green, healthy) to low NDVI (senescence, yellow/brown), which must be distinguished from pest-related declines. Pest-related NDVI declines are more gradual and associated with specific temporal patterns linked to pest life cycles and feeding behavior.

4.2.2 Time-Series Vegetation Indexes Analysis

Figures 6 and 7 present the mean NDVI and LAI time-series comparisons between FAW-infested and healthy maize crops in Southern India. We observe on both plots that the FAW-infested field exhibits a significant decline in NDVI and LAI values. Because NDVI and LAI are indicators of biomass, this decline reflects the damage caused by FAW feeding on the maize plants, leading to reduced leaf area and overall plant health.

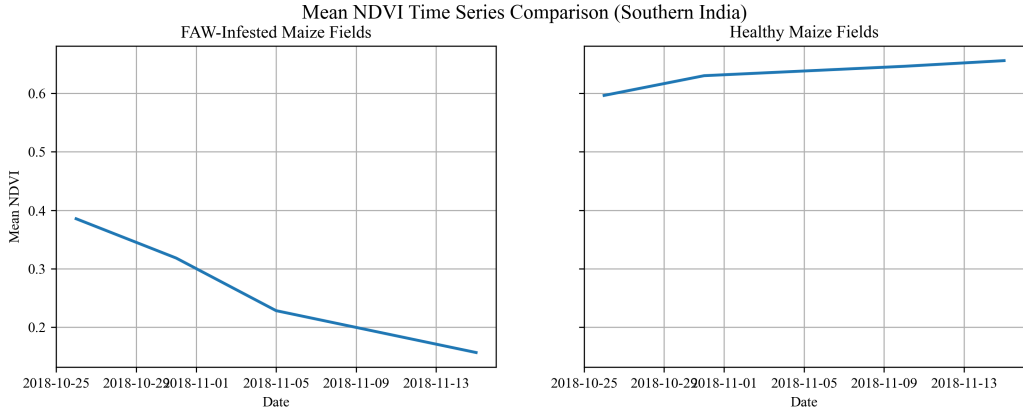


Figure 6: Mean NDVI time series comparison between FAW-infested and healthy maize crops in Southern India.

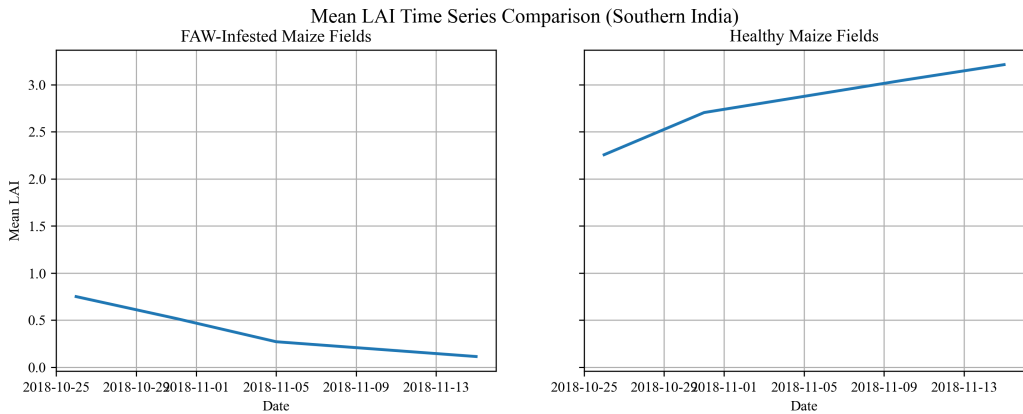


Figure 7: Mean LAI time series comparison between FAW-infested and healthy maize crops in Southern India.

Figures 8 and 9 show the NDVI and LAI time-series maps of the FAW-infested field in Southern India. In both figures, we observe a clear temporal decline in NDVI and LAI values across the field, corresponding to the period of FAW infestation. The spatial patterns in these maps highlight the extent and severity of the damage caused by the pest, with lower index values indicating areas of more severe infestation and biomass loss.

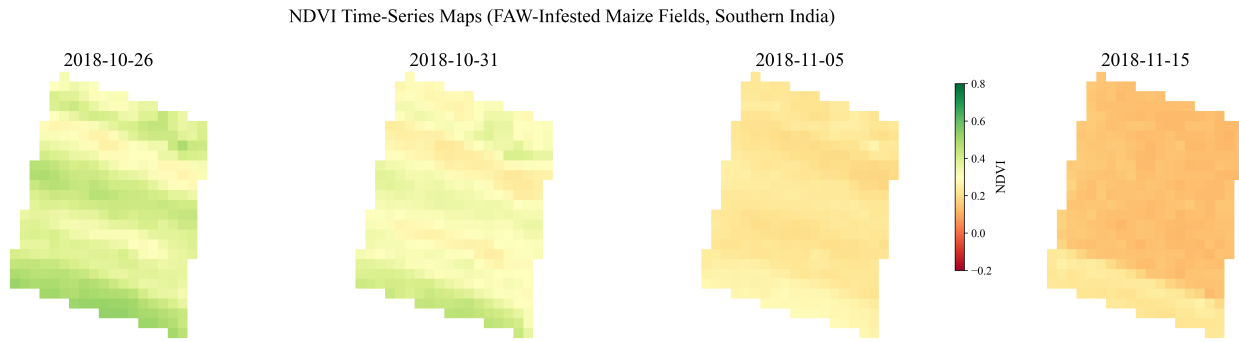


Figure 8: NDVI time series of FAW-infested in Southern India.

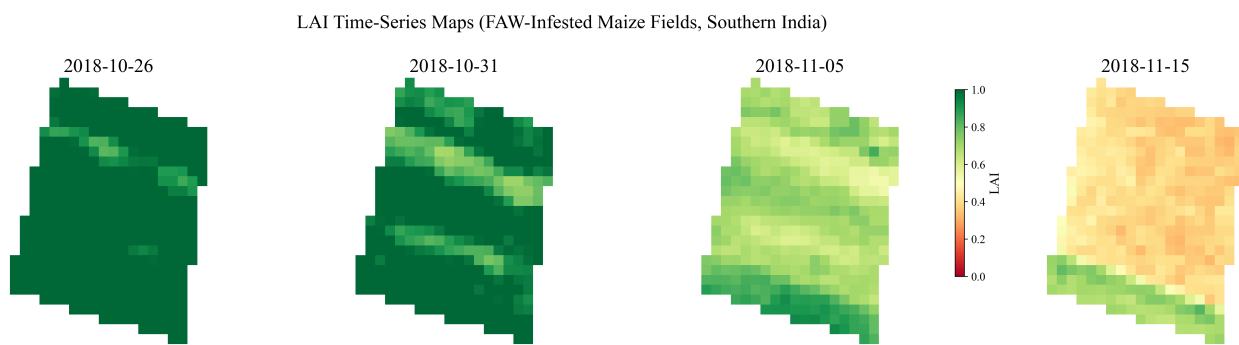


Figure 9: LAI time series of FAW-infested in Southern India.

We can extend the result to more dates. Figure

4.2.3 Temporal Anomaly Detection

5 Conclusion and Future Work

References

1. Boegh, E., Søgaard, H., Broge, N. H., Hasager, C. B., Jensen, N. O., Schelde, K., & Thomsen, A. (2002). Airborne multispectral data for quantifying leaf area index, nitrogen concentration, and photosynthetic efficiency in agriculture. *Remote Sensing of Environment*, 81(2–3), 179–193. [https://doi.org/10.1016/S0034-4257\(01\)00342-X](https://doi.org/10.1016/S0034-4257(01)00342-X)
2. Bilintoh, T.M., et al. (2019). Impact of Armyworm infestations on crops in Ghana: Field validation study.
3. Huete, A., et al. (1997). Overview of the radiometric and biophysical performance of the MODIS vegetation indices. *Remote Sensing of Environment*.
4. Mudereri, B.T., et al. (2022). Application of remote sensing indices for crop health assessment. *Journal of Agricultural Science*.
5. Rouse, J.W., et al. (1974). Monitoring vegetation systems in the Great Plains with ERTS. *Third ERTS Symposium*.
6. Torgbor, B.A., et al. (2022). Remote sensing for pest detection in smallholder agriculture. *Remote Sensing Applications*.
7. Weiss, M., and Baret, F. (2016). S2ToolBox Level 2 products: LAI, FAPAR, FCOVER. *ESA Sentinel-2 Documentation*.
8. Zamanzadeh Darban, Z., et al. (2024). Time series anomaly detection: Methods and applications. *Pattern Recognition*.
9. Zheng, Q., et al. (2018). A review of remote sensing applications in pest and disease detection. *Computers and Electronics in Agriculture*.

Online Resources

1. Time Series Smoothing Methods Tutorial. Kaggle.
kaggle.com/code/furkannakdagg/time-series-smoothing-methods-tutorial
2. Smoothing Techniques for Time Series Data. Medium.
medium.com/@srv96/smoothing-techniques-for-time-series-data
3. Introduction to Time Series Forecasting: Smoothing Methods. Medium/Codex.
4. Makerere Fall Armyworm Crop Challenge. Zindi Africa.
zindi.africa/competitions/makerere-fall-armyworm-crop-challenge